

## Stagnation Pressure of Imploding Shells and Ignition Energy Scaling of Inertial Confinement Fusion Targets

A. Kemp and J. Meyer-ter-Vehn

Max-Planck-Institut für Quantenoptik, D-85748 Garching, Germany

S. Atzeni

Dipartimento di Energetica, Università di Roma 'La Sapienza' and INFN, I-00161 Roma, Italy

(Received 24 November 2000)

The stagnation pressure  $p_s$  of imploding cylindrical ( $n = 2$ ) and spherical ( $n = 3$ ) shells is found to scale as  $p_s/p_0 \propto M_0^{2(n+1)/(\gamma+1)}$ , where  $M_0$  is the Mach number of the imploding shell and  $p_0$  its maximum pressure. The result holds approximately for Mach numbers in the range  $2 < M_0 < 25$  relevant for inertial confinement fusion capsules and is of key importance for their ignition energy scaling. It is derived analytically on the basis of similarity solutions for an ideal gas with adiabatic exponent  $\gamma$ .

DOI: 10.1103/PhysRevLett.86.3336

PACS numbers: 52.57.Bc, 47.40.-x, 52.35.Tc

Inertial confinement fusion (ICF) relies on the implosion of spherical shells to ignite enclosed fuel. The shells are driven by external beams. In a recent paper [1], Herrmann *et al.* report a new scaling law for the minimum ignition energy of ICF capsules

$$E_{\text{ign}} \propto \alpha_{\text{if}}^{1.88 \pm 0.05} p_0^{-0.77 \pm 0.03} v_{\text{imp}}^{-5.89 \pm 0.12} \quad (1)$$

in terms of the in-flight adiabat  $\alpha_{\text{if}}$  of the shell at peak implosion velocity  $v_{\text{imp}}$  and drive pressure  $p_0$ . The adiabat parameter  $\alpha = p/p_{\text{deg}}$  denotes the pressure of the compressed fuel shell relative to that of a fully degenerate Fermi gas at the same electron density. Formula (1) has been extracted from a large number of implosion simulations. In the present paper, we interpret it by means of a similarity solution [2] and derive the underlying theory analytically.

The similarity solution describing the implosion of a hollow spherical gas shell is shown in Fig. 1 in terms of fluid trajectories in a radius-time diagram. Insets illustrate typical density profiles close to the time of void closure ( $t = 0$ ). In ICF implosions, ignition and burn occur when the imploding fuel stagnates behind the shock emerging from the center after void closure. Notice in Fig. 1 that the fuel is almost isobaric in this region.

The main result of this paper is that the ratio  $p_s/p_0$  of fuel pressures at times of stagnation and void closure is the same for each fluid element and depends almost exclusively on the Mach number  $M_0$  of the imploding shell. For a spherical gas shell with adiabatic exponent  $\gamma = 5/3$ , one finds

$$p_s/p_0 \propto M_0^3. \quad (2)$$

ICF ignition requires that temperature  $T_s$  and density-radius product  $\rho_s R_s$  of the hot spot, centrally igniting the stagnating fuel, exceed certain values. Treating, in particular, the product  $p_s R_s \propto \rho_s R_s T_s$  as an invariant, set by fusion physics, one finds that the hot spot energy  $E_s \propto p_s R_s^3 = (p_s R_s)^3 / p_s^2$  scales  $\propto p_s^{-2}$ . This is a key assumption of the isobaric ignition model [3], which well

reproduces simulation results. The model also implies that  $E_s$  is a fixed fraction of the total fuel energy  $E_{\text{ign}}$  for optimal conditions, and this leads to

$$E_{\text{ign}} \propto p_s^{-2} \propto p_0^{-2} M_0^{-6} \propto \alpha_{\text{if}}^{1.8} p_0^{-0.8} v_{\text{imp}}^{-6}, \quad (3)$$

making use of Eq. (2),  $M_0 = v_{\text{imp}}/c_{\text{if}}$ ,  $c_{\text{if}}^2 \propto p_0/\rho_0$  and  $\alpha_{\text{if}} \propto p_0/\rho_0^{5/3}$ , where  $p_0$  and  $\rho_0$  are now identified with peak pressure and density of the shell.

The intriguing coincidence of Eqs. (1) and (3) has triggered the present work. Formula (1) is based on state-of-the-art ICF simulations accounting for real materials and

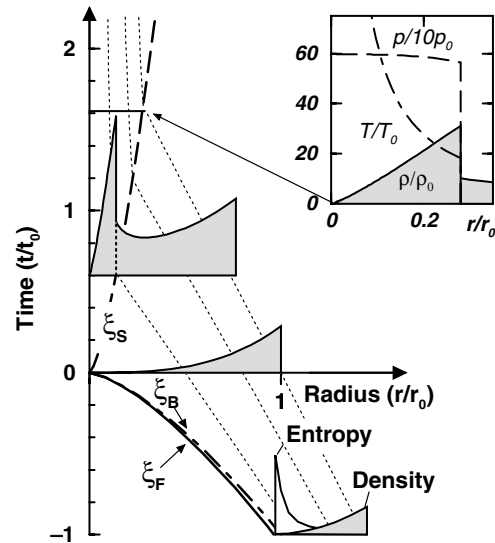


FIG. 1. Self-similar solution of a spherically imploding shell in a  $r, t$  diagram for  $\alpha = 0.7$ ,  $\kappa = 3$ , and  $\gamma = 5/3$ . The inner surface of the shell ( $\xi_F = 0.96$ ) and trajectory of rebounding shock ( $\xi_S = 0.198$ ) are represented by thick  $\xi = r/t^\alpha$  lines. The  $t = 0$  axis corresponds to  $\xi = \infty$ . Fluid elements move on dotted trajectories with almost constant velocity. Insets show density profiles at different times; also shown are entropy at  $t/t_0 = -1$  as well as pressure and temperature distributions at  $t/t_0 = 1.6$ . Normalization is such that sonic point  $B$  is at  $\xi_B = r_0/t_0^\alpha = 1$ ;  $\rho_0$ ,  $T_0$ , and  $p_0$  refer to the fluid element at  $r = r_0$  and  $t = t_0$ , which is considered as an outer boundary.

energy transport, while Eq. (3) is restricted by ideal gas dynamics (no transport) and highly idealized boundary conditions. The crucial relation is Eq. (2) which had been obtained before in [2], but only as a numerical side result. Here we derive it analytically in general form for both cylindrical and spherical geometry and arbitrary  $\gamma$ .

The basic analysis is that of Guderley [4] studying centrally converging shock waves and that has been outlined at several places in the literature; see, e.g., Ref. [2]. It postulates universal behavior of imploding flows near the center of convergence and that interfaces such as the shell's inner surface ( $\xi_f$ ) and the rebounding shock ( $\xi_s$ ), see Fig. 1, run on trajectories  $R = \xi t^\alpha$ , characterized by a constant  $\xi$  and an exponent  $\alpha$ . Corresponding velocities are  $u = dR/dt = \alpha R/t$  and prompt the similarity ansatz

$$\begin{aligned} u(r, t) &= (\alpha r/t)U(\xi), & c(r, t) &= (\alpha r/t)C(\xi), \\ \rho(r, t) &= r^\kappa G(\xi), & \xi &= r/|t|^\alpha, \end{aligned} \quad (4)$$

for the hydrodynamic fields of velocity  $u(r, t)$ , sound velocity  $c(r, t)$ , and density  $\rho(r, t)$ . The essential feature of this ansatz is that the similarity coordinate  $\xi$  and the reduced functions  $U(\xi)$ ,  $C(\xi)$ , and  $G(\xi)$  are invariants with respect to scale transformations of time, radius, and mass. The corresponding scaling group [5] contains the exponents  $\alpha$  and  $\kappa$  as free parameters.

Ansatz (4) has some immediate consequences. It implies that, at the time of void closure  $t = 0$  ( $\xi = \infty$ ), all hydrodynamic functions are represented by power laws

$$\begin{aligned} u(r, 0) &= u_0 r^{-\lambda}, & c(r, 0) &= c_0 r^{-\lambda}, \\ \rho(r, 0) &= \rho_0 r^\kappa, \end{aligned}$$

with  $\lambda = 1/\alpha - 1$  and front factors obtained from (4) with  $t = (r/\xi)^{1/\alpha}$  in the limit  $\xi \rightarrow \infty$ . Note that the flow is characterized by uniform Mach number  $M_0 = u_0/c_0$  at  $t = 0$ . At the same time, the entropy distribution  $A(r, t = 0) = p/\rho^\gamma = A_0 r^{-\epsilon}$  is determined by the exponent  $\epsilon = \kappa(\gamma - 1) + 2\lambda$ . For  $\epsilon > 0$ , entropy diverges in the center, similar to that of stagnating ICF fuel. The entropy distribution at  $t/t_0 = -1$  is indicated in Fig. 1. In the following,  $M_0$  and  $\epsilon$  are used to characterize the imploding shells rather than the equivalent parameters  $\alpha$  and  $\kappa$ . As it turns out, self-similar solutions exist for a continuous range of  $M_0$  and  $\epsilon$  values.

Another consequence of Eq. (4) refers to trajectories  $R(t, a)$  of particular fluid elements  $a$ , depicted in Fig. 1 by dotted lines. They are determined by

$$d \ln R / d \ln \xi = U(\xi) / [U(\xi) - 1], \quad (5)$$

following directly from  $dR/dt = u(R, t) = (\alpha R/t)U(\xi)$ , where  $R(\xi, a)$  is now interpreted as a function of  $\xi$  and time follows from  $t(\xi, a) = (R/\xi)^{1/\alpha}$ . Integrating Eq. (5) from  $\xi_1$  to  $\xi_2$  for a given  $a$ , we find that ratios  $R(\xi_2, a)/R(\xi_1, a)$  do not depend on which fluid trajectory is considered, but are the same for each element  $a$ . Because of relations (4), the same is true for ratios of density, pressure, and other physical quantities. Choosing  $\xi_1 = \infty$

( $t = 0$  axis) and  $\xi_2 = \xi_s$  (rebounding shock), one obtains the important result that the ratios  $\rho_s/\rho_0$ ,  $p_s/p_0$ , etc. are the same for all fluid elements. These final enhancements of density and pressure during shell stagnation represent the central issue of this paper. As we shall see, they depend almost exclusively on the Mach number  $M_0$ , but very little on the entropy distribution.

The explicit solution is derived from the equations of ideal gas dynamics

$$\begin{aligned} \partial_t \rho + \partial_r(\rho u) + (n-1)\rho u/r &= 0, \\ \partial_t u + u \partial_r u + (1/\rho) \partial_r p &= 0, \\ \partial_t(p/\rho^\gamma) + u \partial_r(p/\rho^\gamma) &= 0, \end{aligned} \quad (6)$$

involving no transport processes. The ideal gas equation of state is used with pressure  $p = \rho c^2/\gamma$ . Entropy is conserved except across shock boundaries. These equations are invariant under the scaling group. For the scale-invariant solutions (4), they reduce to the ordinary differential equations [2]

$$\begin{aligned} a_1 dU + b_1 dC + d_1 d \ln \xi &= 0, \\ a_2 dU + b_2 dC + d_2 d \ln \xi &= 0, \end{aligned} \quad (7)$$

with coefficients  $a_1 = C/\mu$ ,  $a_2 = U - 1$ ,  $b_1 = U - 1$ ,  $b_2 = \mu C$ ,  $d_1 = C[U(1 + n/\mu) - 1/\alpha]$ ,  $d_2 = U(U - 1/\alpha) + C^2\{\mu + (\kappa + \mu\lambda)/[\gamma(1 - U)]\}$ , and  $\mu = 2/(\gamma - 1)$ . The coefficients are independent of  $G$  and space-time variables  $r$ ,  $t$ , and  $\xi$ . The problem therefore reduces to the single ordinary differential equation

$$dU/dC = \Delta_1(U, C)/\Delta_2(U, C) \quad (8)$$

giving solutions  $U(C)$ ; the  $\xi$  dependence is then obtained by quadrature of

$$d \ln \xi / dC = \Delta_0(U(C), C)/\Delta_2(U(C), C), \quad (9)$$

where the determinants are given by  $\Delta_0 = a_1 b_2 - b_1 a_2$ ,  $\Delta_1 = b_1 d_2 - d_1 b_2$ , and  $\Delta_2 = d_1 a_2 - a_1 d_2$ .

The imploding shell solution, shown in Fig. 1, is given as the thick solid curve in the  $U, C$  plane of Fig. 2. A unique feature is that it describes the implosion both before and after void closure. The branch  $OBF$  corresponds to the imploding shell ( $t < 0$ ), while the branch  $OS_1 S_2 E$  refers to the shell after void closure ( $t > 0$ );  $OS_1$  describes the outer part still imploding,  $S_1 S_2$  the shock front emerging from the center, and  $S_2 E$  the gas stagnating in the center behind the shock front. Points  $O$ ,  $B$ , and  $D$  are singular points, for which  $dU/dC \rightarrow 0/0$ . From Eq. (9) one finds that  $\xi \rightarrow \infty$  at point  $O$ . It therefore describes the outer part of the imploding shell, and the slopes of the solution curves  $OB$  and  $OS_1$  close to  $O$  are equal to the Mach number  $M_0 = U/C$ .

We emphasize that the imploding shell solution presented here is almost identical to the imploding shock solution first discussed by Guderley in [4]. In both cases, the  $t < 0$  branch has to cross the sonic line  $C = 1 - U$  at singular point  $B$  (crossing it at other points would lead

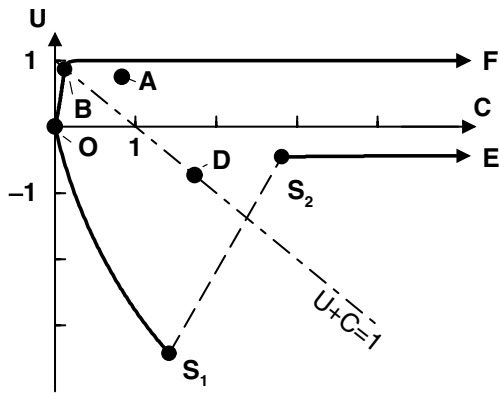


FIG. 2. Self-similar solution of Fig. 1 in a  $U, C$  plane. Dots  $O, B, D$ , and  $E, F$  located at  $C \rightarrow \infty$  represent singular points, where  $dU/dC \rightarrow 0/0$ . The solid curve  $OBF$  corresponds to the imploding shell for  $t < 0$  and curve  $OS_1S_2E$  to the gas for  $t > 0$  after void closure; they match at point  $O$  where  $\xi = r/|t|^\alpha = \infty$ ; it describes the solution at  $t = 0$ , and also outer gas layers at  $r \rightarrow \infty$  for  $|t| \neq 0$ . The jump  $S_1S_2$  describes the rebounding shock at  $\xi_s$ , and  $S_2E$  the stagnating gas at  $0 \leq \xi \leq \xi_s$ .

to double-valued, nonphysical solutions). For Guderley's shock converging in uniform gas, implying  $\kappa = 0$ , the solution has to satisfy strong shock conditions at the inner boundary; i.e., it has to hit the strong shock point at  $U_A = 2/(\gamma + 1)$ ,  $C_A = \sqrt{2\gamma(\gamma - 1)/(\gamma + 1)}$ , and this singles out a unique value of  $\alpha$ . On the other hand, the imploding shell solutions considered here have to reach the inner surface point  $F$  at  $U_F = 1$  and  $C_F = \infty$ , and this is possible for a continuous set of  $\alpha$  and  $\kappa$  values [2]. Crossing the sonic point  $B$ , however, is of deep significance also in the present context, because it determines the Mach number  $M_0$  of the imploding shell as a function of  $n, \gamma, \alpha$ , and  $\kappa$ ; see Eq. (15).

After void closure, the imploding shell is converted into the stagnated gas behind the rebounding shock. Remarkably, this state can be derived analytically from Eqs. (8) and (9). It is described by the separatrix running toward the singular point  $E$  at  $U_E = -(\kappa - 2\lambda)/n\gamma$  and  $C_E \rightarrow \infty$ , where  $\xi_E = 0$ . The explicit solution, valid asymptotically for  $r \rightarrow 0$  and  $t > 0$ , is

$$\begin{aligned} u(r, t) &= -\alpha(\kappa - 2\lambda)/(n\gamma)r/t, \\ \rho(r, t) &\propto r^{n\epsilon/\nu} t^{\alpha(\kappa - n\epsilon/\nu)}, \\ p(r, t) &\propto r^0 t^{\alpha(\kappa - 2\lambda)}, \end{aligned} \quad (10)$$

with  $\nu = n\gamma + \kappa - 2\lambda$ . For  $\epsilon > 0$ , the density vanishes in the center, while the temperature  $T \propto c^2$  diverges such that the pressure  $p \propto \rho T$  is uniform. In the special case of  $\kappa = 2\lambda$ , these asymptotic results hold even globally and describe an isobaric gas at rest. In this case, the solution branch  $S_2E$  coincides with the  $U = 0$  axis in Fig. 2. The locations of the shock points  $S_1$  and  $S_2$  are obtained from the Hugoniot relations; see [2].

The goal of the present paper is to study the ratios of pressure  $p_s/p_0$  and also density  $\rho_s/\rho_0$  as functions of Mach number  $M_0$  and entropy parameter  $\epsilon$ . Numerical

results, obtained for a set of  $\alpha$  and  $\kappa$  values chosen to cover the range of  $2 < M_0 < 25$  and  $0.3 < \epsilon < 6$ , are plotted versus  $M_0$  in Fig. 3. For spherical shells ( $n = 3$ ) of  $\gamma = 5/3$  gas, the results are well represented by  $p_s/p_0 \approx 3.6M_0^3$  and  $\rho_s/\rho_0 \approx 2.4M_0^{3/2}$ . For different  $\epsilon$  at fixed  $M_0$ , pressure and density ratios are almost identical. It appears that the final compression ratios depend strongly on the Mach number of the imploding shell, but are rather independent of the entropy distribution. This remarkable result will now be derived analytically.

Presuming large Mach numbers  $M = U/C \gg 1$ , we find the approximate integral

$$M \cong M_0[(1 - U)/(1 - \alpha U)^n]^{1/\mu} \quad (11)$$

of Eq. (8) for solution curves starting at point  $O$ . We apply it to branch  $OB$  to determine  $M_0$  and also to branch  $OS_1S_2$  for getting  $\rho_s/\rho_0$  and  $p_s/p_0$ . Strong shock relations are used to describe the jump  $S_1S_2$ . Adiabatic compression of fluid elements between void closure (point  $O$ ) and the time of the shock passage (point  $S_1$ ) satisfies  $\rho \propto c^\mu$ . Note also that fluid elements move at almost constant velocity during this period [derive  $d \ln u/d \ln \xi \cong 0$  from Eqs. (4)–(9) and compare Fig. 1]. This leads to  $c \propto 1/M$  and  $\rho_1/\rho_0 \cong (1 - \alpha U_1)^n/(1 - U_1) \cong \alpha^n(1 - U_1)^{n-1}$ , valid for  $(1 - U_1) \gg 1$ . Invoking also strong shock compression

$$\rho_s/\rho_1 = (1 - U_1)/(1 - U_2) \cong \Gamma \quad (12)$$

with  $\Gamma = (\gamma + 1)/(\gamma - 1)$ , we find the total compression ratio

$$p_s/p_0 = (\rho_s/\rho_1)(\rho_1/\rho_0) \cong (\alpha\Gamma)^n(1 - U_2)^{n-1}. \quad (13)$$

Indices 1 and 2 refer to  $S_1$  and  $S_2$ , respectively. Similarly, the final pressure ratio can be split up into the adiabatic

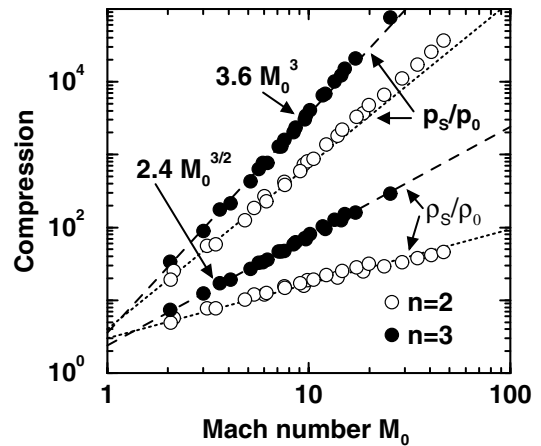


FIG. 3. Compression ratios  $p_s/p_0$  and  $\rho_s/\rho_0$  of fluid elements between times of void closure (index 0) and passage of rebounding shock (index  $s$ ) plotted versus Mach number  $M_0$ . Dots represent numerical solutions of the similarity model and lines refer to analytical scaling formulas (open dots correspond to cylindrical, full dots to spherical geometry). The small scatter of the results around the power laws reflects different values of the entropy parameter  $\epsilon$ .

contribution  $p_1/p_0 = (\rho_1/\rho_0)^\gamma$  and the strong shock contribution  $p_s/p_1 \cong 2\gamma/(\gamma + 1)[(1 - U_1)/C_1]^2$ . Combining these relations with Eqs. (11) and (12), one obtains

$$\frac{p_s}{p_0} \cong \frac{2\gamma}{\gamma - 1} \frac{(1 - U_2)^{n+1}}{[1 - \Gamma(1 - U_2)]^2} (\alpha\Gamma)^n M_0^2. \quad (14)$$

We still have to express  $(1 - U_2)$  by  $M_0$ , exploiting the condition that the solution curve in the upper part ( $U > 0$ ) of Fig. 2 crosses the sonic line  $C = 1 - U$  at  $B$ . The positions of the singular points  $B$  and  $D$  are determined by  $\Delta_1(U, 1 - U) = \Delta_2(U, 1 - U) = 0$ . From the resulting quadratic equation for  $U = U_{B,D}$ , one obtains approximately  $U_B \cong 1$ ,  $(1 - \alpha U_B) \cong (1 - \alpha)$ , and  $(1 - U_B) \cong (\lambda/n)/(1 - U_2)$ , where  $U_2 \cong -(\kappa - 2\lambda)/(n\gamma)$  is the velocity at  $S_2$  behind the rebounding shock. Substituting these expressions in Eq. (11), we obtain

$$M_0 \cong (1 - \alpha)^{n/\mu} [n\alpha/(1 - \alpha)]^{1+1/\mu} (1 - U_2)^{1+1/\mu}. \quad (15)$$

Making use of Eq. (15), the density ratio (13) can be written in the form

$$\rho_s/\rho_0 \cong f(\alpha) M_0^{2(n-1)/(\gamma+1)} \quad (16)$$

with  $f(\alpha) = \Gamma^n n^{1-n} \alpha (1 - \alpha)^{(1-n/\Gamma)(n-1)}$ . For typical cases with  $n < \Gamma$ , the front factor  $f(\alpha)$  depends weakly on  $\alpha$  and can be replaced by a constant in the relevant range of  $0.6 < \alpha < 0.9$ , corresponding to  $M_0$  and  $\epsilon$  values covered in Fig. 3. For  $n = 3$  and  $\gamma = 5/3$ , one obtains  $f_{\max} \cong 2.7$  and  $2(n - 1)/(\gamma + 1) = 3/2$  in good agreement with the numerical results in Fig. 3. The pressure ratio (14) is not immediately of power law structure in  $x \equiv 1 - U_2$ , but approximating the function  $F(x) \equiv x^{n+1}/(1 - \Gamma x)^2$  by the power law  $F(x) \approx F_1 x^\sigma$  at  $x = 1$ , one finds  $\sigma = n - \gamma$  and  $F_1 = (\gamma - 1)^2/4$ . This leads to

$$p_s/p_0 \cong g(\alpha) M_0^{2(n+1)/(\gamma+1)}. \quad (17)$$

For  $n = 3$  and  $\gamma = 5/3$ , it reproduces the central scaling relation  $p_s/p_0 \propto M_0^3$ . Again, the front factor  $g(\alpha) = \gamma(\gamma - 1)\Gamma^n n^{\gamma-n} \alpha^\gamma (1 - \alpha)^{(1-n/\Gamma)(n-\gamma)}/2$  is a weak function of  $\alpha$  and can be replaced by its maximum. For  $n = 3$  and  $\gamma = 5/3$ , we find  $g_{\max} \cong 3.4$  in reasonable agreement with the numerical result. From the derivation, it should be clear that the power formula (17) is only of approximate validity in an intermediate range of Mach numbers  $M_0$ . This is also visible in Fig. 3, where the straight-line power law (17) touches tangentially the somewhat curved numerical results. Notice that the fitting

point  $x \equiv 1 - U_2 = 1$  chosen above is the most natural one, because it corresponds to  $U_2 \cong (\kappa - 2\lambda)/n\gamma = 0$ , and therefore to the distinguished special case in which the stagnated gas is uniform and at rest; see Eq. (10). The scaling laws (16) and (17) also describe the numerical solutions in Fig. 3 for cylindrical ( $n = 2$ ) geometry, giving  $p_s/p_0 \propto M_0^{9/4}$  and  $\rho_s/\rho_0 \propto M_0^{3/4}$  for  $\gamma = 5/3$ . The approximation leading to Eq. (17) does not apply to  $n = 1$ ; the case of plane geometry is intrinsically different because there are no convergence effects.

In conclusion, we have derived approximate scaling laws describing pressure and density of cylindrically and spherically converging gas shells when stagnating in the center. They are based on a two-parameter similarity solution of ideal gas dynamics which describes both the imploding shell and stagnation. It turns out that stagnation pressure and density scale almost exclusively with the Mach number of the imploding shell, but are insensitive to its entropy distribution. As the new result, this is derived analytically in general form for cylindrical and spherical geometry and arbitrary  $\gamma$ .

Do the present results apply also to general, non-self-similar implosions? We cannot answer this question on the model basis presented here. In ICF capsule implosions, density and entropy distributions are strongly modified by energy transport and other effects; they are far from being self-similar. The remarkable coincidence, however, of the general scaling law (1) obtained by Herrmann *et al.* [1] and the model result (3) may indicate that the scaling formula (17) has a larger range of validity than the model it is based on. Indeed, the insensitivity with respect to the entropy distribution may imply that the scaling with  $M_0$  holds also for other non-self-similar entropy distributions. It should be a challenge to check this conjecture in more detail.

The authors acknowledge controversial, but helpful discussions with M. Basko on the topic of this paper.

- 
- [1] M. C. Herrmann, M. Tabak, and J. D. Lindl, *Nucl. Fusion* **41**, 99 (2001).
  - [2] J. Meyer-ter-Vehn and C. Schalk, *Z. Naturforsch. A* **37**, 955 (1982); J. Meyer-ter-Vehn, in *Proceedings of the 29th Scottish Universities Summer School in Physics: Laser-Plasma Interactions 3*, edited by M. Hooper (SUSSP Publications and Institute of Physics Publishing, London, 1985), Vol. 14, pp. 234–245.
  - [3] J. Meyer-ter-Vehn, *Nucl. Fusion* **22**, 561 (1982).
  - [4] G. Guderley, *Luftfahrtforschung* **19**, 302 (1942).
  - [5] S. Coggeshall and J. Meyer-ter-Vehn, *J. Math. Phys. (N.Y.)* **33**, 3585 (1992).